TLR4 Response to LPS Is Reinforced by Urokinase Receptor

Yulia Kiyan[1]*, Sergey Tkachuk[1], Song Rong[2], Anna Gorrasi[3], Pia Ragno[4], Inna Dumler[1], Hermann Haller[1] and Nelli Shushakova[1,2]

[1] Nephrology Department, Hannover Medical School, Hannover, Germany, [2] Phenos GmbH, Hannover, Germany, [3] Nouscom, Rome, Italy, [4] Department of Chemistry and Biology, University of Salerno, Salerno, Italy

GPI-anchored uPAR is the receptor for the extracellular serine protease urokinase-type plasminogen activator (uPA). Though uPAR role in inflammatory processes is documented, underlying mechanisms are not fully understood. In this study we demonstrate that uPAR is a part of Toll-like receptor 4 (TLR4) interactome. Downregulation of uPAR expression resulted in diminished LPS-induced TLR4 signaling, less activation of NFκB, and decreased secretion of inflammatory mediators in myeloid and non-myeloid cells *in vitro*. In vivo uPAR−/− mice demonstrated better survival, strongly diminished inflammatory response and better organ functions in cecal ligation and puncture mouse polymicrobial sepsis model. Mechanistically, GPI-uPAR and soluble uPAR colocalized with TLR4 on the cell membrane and interacted with scavenger receptor CD36. Our data show that uPAR can interfere with innate immunity response *via* TLR4 and this mechanism represents a potentially important target in inflammation and sepsis therapy.

Keywords: urokinase receptor, CD36, sepsis, LPS, TLR4

INTRODUCTION

uPAR is the receptor for urokinase-type plasminogen activator (uPA), an extracellular serine protease and important activator of ubiquitous multifunctional protease plasmin. uPAR is anchored to the outer cell membrane leaflet *via* GPI anchor. Binding uPA to uPAR localizes proteolysis at the cell surface to facilitate spatially and temporally restricted activation of plasmin. Wide substrate specificity of plasmin provides for multiple functions of the protease such as fibrin cloth lysis, tissue remodeling, cell migration (1, 2). In addition, uPAR acts independently from the proteolytic activity of uPA. Binding of uPA or its catalytically inactive amino terminal fragment to uPAR or uPAR overexpression induces intracellular signaling pathways orchestrating important cellular functions such as proliferation, differentiation, migration, DNA repair (1, 3, 4). Since uPAR is a GPI anchored protein and lacks a transmembrane domain, it relies on interaction with other receptors to transduce signals across cell membrane. uPAR interaction with several transmembrane receptors, integrins, and ECM components has been demonstrated (1).

uPA/uPAR are expressed by many cells of hematopoietic origin (5) and endothelial cells (6, 7). Expression of uPAR system can be rapidly upregulated in response to bacterial infection or inflammation. Despite the role of uPAR in inflammatory processes attracted attention (8, 9), its role is still not fully understood. Data obtained using uPAR−/− and uPA−/− mice models suggest that

uPAR role in response to bacterial infection and innate immunity can be independent from uPA and its catalytic activity (10, 11). Effects of uPAR are often attributed to the impaired infiltration of immune cells. Thus, uPAR−/− mice showed reduced accumulation of inflammatory cells in the lung upon *Streptococcus pneumoniae and Pseudomonas aeruginosa* infection (10, 11). This was accompanied by stronger propagation of the infection and higher mortality. Interestingly, *S. pneumoniae* caused modest increase in the lung levels of cytokines and chemokines in uPAR−/− mice. *S. pneumoniae* and its cell wall component lipoteichoic acid (LTA) are recognized primarily by TLR2 receptor (12). In another study Liu and coworkers (13) addressed uPAR/TLR2 cross-talk directly. They reported that uPAR−/− neutrophils demonstrate diminished response to TLR2 ligand, PAM3CSK4 during *in vitro* stimulation. mRNA expression of cytokines in response to PAM3CSK4 was unchanged in uPAR−/− cells but the secretion of cytokines was decreased.

Sepsis is a severe and a life threatening condition that is characterized as an inadequate response to infection and multiorgan dysfunction (14, 15). Plasma level of soluble uPAR (suPAR) alone and in combination with other biomarkers serves as a prognostic predictor and a marker in patients with sepsis and systemic inflammatory response (SIRS) (16, 17). We have previously demonstrated that uPAR cooperates with CD36 and TLR4 to mediate signaling induced by binding of oxidated low density lipoprotein (oxLDL) in vascular smooth muscle cells (18). OxLDL is an important Danger Associated Molecular Pattern (DAMP) molecule regulating survival and phenotype of macrophages, endothelial cells, and smooth muscle cells. We demonstrated that downregulation of uPAR in human vascular smooth muscle cells was protective against oxLDL-dependent phenotypic modulation. Scavenger receptor CD36 and innate immune receptor TLR4 also recognize Pathogen Associated Molecular Pattern molecules (PAMPs) such as LPS (19, 20) and play important roles in sepsis. We asked, if uPAR can interfere also with PAMPs signaling and whether interaction of uPAR with these receptors is important *in vivo* in sepsis.

MATERIALS AND METHODS

Materials
Unconjugated and Alexa 647-conjugated anti-mouse uPAR antibody were from R&D Systems (MAB531 and FAB531R, respectively); TLR4 antibody (MAB27591) was from R&D Systems; LPS (L2887) was from Sigma, Biotin-LPS and PAM3CSK4 were from Invivogen; Soluble mouse uPAR was from CinoBiologicals. Human IL-6 and IL-8 ELISAs were from Thermofisher Scientific. Mouse inflammation CBA kit was from BD Biosciences. Mouse and human uPAR siRNA and non-sence siRNA control duplexes were from Santa Cruz Biotechnology. Fluorescein isothiocyanate (FITC) was from Sigma.

RT-PCR
RNA was isolated using RNAEasy kit from Quiagen. TaqMan RT-PCR was performed using TaqMan Master Mix and Light Cycler96 (Roche). Oligonucleotides are listed in **Supplementary Table 1**.

Cell Culture, Transfection, and Luciferase Assay
Immortalized mouse peritoneal mesothelial cell line was generated in our lab by limited dilution cultures of primary cells obtained from omentum tissue of Immorto mice harboring the tsSV40T gene as previously described (21). The cells were propagated in RPMI 1640 cell culture medium containing 1% penicillin–streptomycin, 10% fetal calf serum, 1% insulin/transferrin/selenium A (all from Life Technologies, Carlsbad, CA), 0.4 μg/ml hydrocortisone (Sigma-Aldrich), and 10 U/ml recombinant mouse interferon gamma (Cell Sciences) at 33°C (permissive conditions). The cell lines were identified by the typical cobblestone morphology of confluent monolayers and by positive staining for E-cadherin, ZO-1, α-SMA, and pan-cytokeratin after 3-day culture at 37°C without interferon gamma (non-permissive conditions). Primary peritoneal mouse macrophages were isolated from wild type and uPAR−/− mice as described previously (22).

Raw 264.7 mouse macrophage cell line was from ATCC and cultivated as recommended by the supplier. HK-2 human kidney proximal tubule epithelial cells were from ATCC and cultivated as recommended by the supplier in Keratinocyte Serum Free Medium containing 0.05 mg/ml bovine pituitary extract and 5 ng/ml EGF.

Mesothelial cells were transfected using PolyPlus transfection reagents accordingly to the manufacturer instructions. HK-2 cells were nucleofected using Mirus nucleofection solution and T20 program of nucleofector (Lonza).

Construction of vector for Gaussia luciferase expression under control of NFκB promoter was described elsewhere (18). Activity was measured using GeneCopoeia kits and Tecan Genios multiplate reader.

Ex Vivo Blood Stimulation
WT and uPAR−/− mouse whole blood was collected in EDTA tube. Stimulation was performed with 50 ng/ml LPS for 3 h at 37°C. Then, the blood was centrifuged at 1500 g for 10 min, and plasma was used for cytokine measurement using Cytokine Beads Array (BD Biosciences).

Biotin-LPS Binding, Pull Down, and Western Blotting
To analyze LPS binding, 1 μg/ml Biotin-LPS was added to the cells. After 30 min of incubation, cells were washed and lysed. For Dot Blot analysis, 10 μg of cell lysate protein was applied to nitrocellulose membrane. Membrane was allowed to dry, blocked in 3% BSA, and incubated with Streptavidine-HRP for 1 h at room temperature. After washing, membrane was developed using Versa Doc Gel Documentation system (BioRad) and QuantityOne software. For pull-down assay, cell lysate was incubated with streptavidine magnetic beads. Beads were then washed, SDS electrophoresis and western blotting have been performed.

Immunocytochemistry and Immunohistochemistry
Cells were grown on coverslips and stimulated as indicated. The cells were fixed and processed for immunostaining as we have

previously described. Staining with antibodies was performed for 1 h at room temperature. DAPI was applied for nuclear staining. Duolink proximity assay kit was purchased from Sigma and used as recommended by the supplier.

2.5 micrometer paraffin-embedded tissue sections were stained with the Alexa-647–conjugated antibodies for mouse uPAR (R&D Systems) and TLR4 followed by Alexa488 conjugated secondary antibodies (ThermoFischer Scientific) were used. All the images were using Leica TCS-SP2 AOBS confocal microscope (Leica Microsystems) oil-immersed ×40 objective, NA 1.25 and ×63 objective, NA 1.4.

Animal Experiments

All procedures were performed in accordance with international guidelines on animal experimentation and approved by the local committee for care and use of laboratory animals (Lower Saxony Office for Consumer Protection and Food Safety). Experiments were performed as previously described (23). Briefly, wild type C57BL/6J and uPAR−/− B6.129P2-*Plaurtm1Jld*/J male mice (20 to 25 g) obtained from Charles River Laboratories (Sulzfeld, Germany) were anesthetized with isofluorane (induction of 3%, maintenance of 1.5%, and oxygen flow of 3 L/min). A 1-cm ventral midline abdominal incision was made and the cecum was ligated with 4-0 silk sutures distal to the ileocecal valve and punctured through with a 24-gauge needle. 1- to 2-mm droplet of fecal material was expelled. The incision was closed using 4-0 surgical sutures. Mice were fluid-resuscitated with 500 μl pre-warmed normal saline intraperitoneally immediately after the procedure. Sham animals underwent the same procedure except for CLP. For postoperative analgesia Butorphanol in a dose of 1 mg/kg body weight was injected subcutaneously before the surgery. In addition metamizol was given p.o. for 3 following days in a dose 200 mg/kg. We did not use antibiotic treatment to avoid its possible effect on investigated parameters.

In this study we used a high-grade sepsis model for short time experiment with follow-up 20 h and a mid-grade sepsis model for survival experiments with follow-up 21 days. For high-grade sepsis model the cecum was ligated distal to the ileocecal valve (75% of the cecum length was ligated) and for mid-grade medium cecal ligation was performed, which comprises 50% to 60% of the cecum, resulting in an expecting survival rate of 40% (24). In both short time and survival experiments 4 groups of mice were used: sham operated WT mice (n=6), CLP operated WT mice (n=10), sham operated uPAR−/− mice (n=10), CLP operated uPAR−/− mice (n=10).

In short-time experiments mice were anesthetized for blood sampling with isofluorane and subsequently sacrificed at 20 h after CLP or sham surgery. Subsequently, peritoneal lavage (PL) was performed with 3 mL of PBS. The volume of the collected PL was measured in each sample, and the total white blood cell count and inflammatory cell populations in PLs were analyzed by Scill Vet abc hematology analyzer (Scil animal care). Serum markers of acute kidney failure (serum creatinine and blood urea nitrogen) and serum markers of acute liver failure (aspartate aminotransferase (AST) and alanine aminotransferase (ALT) activities) as well as lactate dehydrogenase activity as a common marker of acute injury were measured in serum samples using an Olympus AU 400 analyzer (Beckman Coulter Inc.),. Serum and PL levels of IL-6, IL-10, MCP-1, TNFα, IFNγ, and IL-12p70 were examined by bead-based flow cytometry assay (CBA Kit; BD Biosciences) in accordance with the instructions of the manufacturer.

Bacterial load in PL 20 h after surgery was analyzed by plating serial dilution of PL fluid on Columbia blood-agar base plates (Biorad).

Functional Analysis of Mouse Resident Peritoneal Macrophages *In Vitro*

Mouse resident PMs were obtained from untreated WT or uPAR −/−mice by PL by using 10 mL of PBS (2 × 5 mL). The cells were centrifuged at 300g for 10 min at 4°C, the supernatants were decanted, and the cell pellets were washed twice with RPMI 1640 medium. Cells were re-suspended in RPMI 1640 medium supplemented with 10% fetal calf serum (FCS) and plated in 24-well plastic culture plates (Corning Inc.) to achieve a final concentration of 1.5×10^6 cells/mL per well. The plates were incubated overnight at 37°C, 5% CO_2, and 95% humidity to allow macrophage adherence. Non-adherent cells were removed by vigorous washing with RPMI 1640 medium. Cells were stimulated with 50 ng/ml LPS for 3 h.

For analysis of macrophage phagocytic activity the *Escherichia coli* strain DH5α was grown in the LB medium (1% trypton, 0.5% yeast extract, 1% sodium chloride) on a reciprocal shaker (150 rpm) overnight at 37°C. After harvesting by centrifugation, bacteria were washed twice with a 0.01 M phosphate buffer in 0.15 M saline (PBS), pH 7.4, once with distilled water, and heat-inactivated for 60 min at 56°C in a water bath. 1×10^9 *E. coli* were further incubated for 60 min in 2.5 ml of 0.1 M carbonate-bicarbonate buffer, pH 9.0, at 4°C; the buffer was supplemented with 500 μg of isomer 1 of fluoresceinisothiocyanate (FITC). After vigorous washing with PBS, fluorescein-labeled *E. coli* cells were opsonized by incubation for 1 h at 37°C with 5% mouse serum. After opsonization, the cells were washed with PBS.

Fluorescein-labeled *E. coli* cells were added to the adherent macrophages that were left untreated or treated with PL obtained from CLP-WT mice 20 h after surgery at a concentration of 5×10^5/ml. After incubation at 37°C for 30 min, phagocytic cells were washed 3 times with PBS and fluorescence was measured using Tecan multiplate reader. Then, cells were fixed with 3% PFA, the plate was allowed to dry and 0.5% trypan blue was added to quantify the number of cells in each well. Excess of trypan blue was washed away and 1% SDS was added to solubilize the trypan blue stained cells. The plate was read at 595 nm sing Tecan multiplate reader. The Fluorescence reading was normalized by the OD of trypan blue staining.

Statistics

Data are presented as mean ± standard deviation (SD). The D'Agostino and Pearson omnibus normality test was used to test for normality. Multiple comparisons were analyzed by two-way ANOVA with Sidak's *post hoc* correction or the Kruskal–Wallis nonparametric test with Dunn's *post hoc* correction. P-values<0.05 were considered statistically significant. GraphPad Prism 8.3.0 (GraphPad Software) was used for data analysis.

RESULTS

uPAR–/– Myeloid Cells Are Less Responsive to LPS Stimulation

Whole blood collected from wild type (WT) and uPAR –/– mice was stimulated ex vivo with LPS from *E. coli*. After optimization of the stimulation conditions (**Supplementary Figure 1**), the release of cytokines was assessed after 3 h of the blood stimulation with 50 ng/ml LPS using the Cytometric Bead Array and flow cytometry. As shown in **Figure 1**, LPS stimulation resulted in strongly increased levels of TNFα and IL-6 in plasma. However, this up-regulation was significantly decreased in the blood obtained from uPAR–/– in comparison to WT mice. The expression of IFNγ was also decreased in uPAR–/– blood though the difference has not reached the significance level (**Supplementary Figure 1B**). The expression of MCP-1 and IL-12p70 were not increased by LPS and were similar in WT and uPAR–/– blood (**Supplementary Figure 1B**). There was a strong trend for increased IL-10 release after ex vivo LPS stimulation of uPAR-/whole blood compared to WT whole blood though the difference was not statistically significant (p=0.0812, two-way ANOVA analysis) (**Figure 1A**). Accordingly, IL6/IL-10 ratio was strongly decreased in uPAR–/– mice suggesting that knock-out blood cells demonstrated less inflammatory response.

The whole blood response to LPS is initially mediated by the response of monocytic cells and largely mediated by TLR4 (25). Therefore, the model of the blood stimulation with LPS ex vivo implies uPAR participation in inflammatory signaling of TLR4 expressing monocytic cells. To investigate this opportunity further, we isolated primary peritoneal macrophages from uPAR–/– and WT mice. As shown in **Figure 1B**, uPAR–/– macrophages demonstrated significantly decreased expression of IL-6, TNFα, and MCP-1 and up-regulated expression of IL-10 after LPS stimulation compared to WT cells. Similar to whole blood stimulation, IL-6/IL-10 ratio was strongly decreased in uPAR–/– macrophages.

To assess the ability of uPAR to associate with proteins of TLR4 interactome, peritoneal macrophages from uPAR–/– mice were treated with mouse suPAR. Then the cells were fixed and stained for confocal microscopy. As shown in **Figure 2A**, in the presence of LPS suPAR also colocalized with membrane TLR4. Despite the ability to associate with TLR4 interactome, suPAR by itself had not induced any significant expression of IL-6 and TNFα in primary WT and uPAR–/– macrophages (**Figure 2B**). However, suPAR promoted LPS response in uPAR–/– cells (**Figure 2B**) confirming that suPAR can integrate into TLR4 interactome and this integration can have physiological relevance in LPS-induced response.

Similar LPS-dependent co-localization of uPAR with TLR4 was observed using confocal microscopy in mouse Raw 264.7 macrophage cell line. These cells have been selected due to their high expression level of TLR4 and uPAR and demonstrate strong LPS response. As shown in **Figure 2C**, in unstimulated cells uPAR and TLR4 located in close proximity. In the presence of LPS, increased colocalization of the receptors was observed. This was further confirmed by biotin-LPS pull down assay performed

in Raw 264.7 cells (**Figure 2D**) - uPAR was found in the protein complex precipitated by biotin-LPS.

Together, this data showed that in the presence of LPS uPAR can integrate into signaling complex of TLR4 and promote the inflammatory response of myeloid cells.

LPS Response of uPAR–/– Non-myeloid Cells Is Impaired

Non-myeloid cells also express TLR4 and its co-receptors and play important role in innate immunity response (26). Mesothelial epithelium covers the internal body cavities and organs, and poses the first line of defense in abdominal bacterial sepsis. The expression of TLR4 by mouse mesothelial epithelial cells and their response to LPS have been reported (27). In our experiments immortalized mouse mesothelial epithelial cells demonstrated a strong response to LPS by high upregulation of IL-6, TNFα, MIP-2, and MCP-1. We transfected mesothelial cells with control and murine uPAR siRNA (**Figure 3A**) and assessed their response to LPS in vitro. As shown in **Figure 3B**, the inflammatory response of uPARsi mesothelial cells was strongly impaired and the expression of IL-6, TNFα, MIP-2 (CXCL2), and MCP-1 was decreased in comparison to the control cells.

To assess mechanisms of uPAR interference with LPS-induced signaling, we investigated protein tyrosine phosphorylation in uPARsi mesothelial cells. As shown in **Figures 3C, D**, tyrosine phosphorylation of multiple proteins was diminished in the absence of uPAR. In particular, phosphorylation of NFκB p65 was strongly decreased.

One of the most vulnerable organs affected by sepsis is the kidney. Recent data demonstrated that kidney tubular epithelial cells participate in immune response, express TLR4 and respond to LPS by expression of inflammatory cytokines (28). To investigate the role of uPAR in the inflammatory response of kidney tubular cells we downregulated uPAR expression in human kidney proximal tubular epithelial cell line HK-2 by means of cell nucleofection with siRNA. HK-2 cells nucleofected with control Si RNA (SiCo) expressed IL-6 and IL-8 in response to LPS treatment. Similar to the above data, we observed strong downregulation of cell response to LPS in uPARsi cells at mRNA and protein level (**Figures 4A, B**).

TLR4 mediates not only signaling induced by PAMPs but is also involved in the recognition of danger associated molecular pattern molecules (DAMPs). One of the important DAMPs is HMGB1 - a DNA binding protein that can be released from damaged cells under stress and activate tubular epithelial cells by interacting with TLR4 in sepsis (29). In HK-2 cells HMGB1 also induced increased expression of IL-6 and IL-8. Similar to LPS, this response was abrogated in uPARsi cells (**Figure 4C**).

To assess effects of uPAR on LPS-dependent NFκB activation, we infected HK-2 cells with lentivirus to express Gaussia luciferase under control of NFκB-dependent promoter. Gaussia luciferase activity assay showed that LPS-dependent regulation of NFκB-sensitive promoter is dependent on uPAR expression (**Figure 4D**) whereas GAPDH promoter is regulated independently on uPAR and LPS.
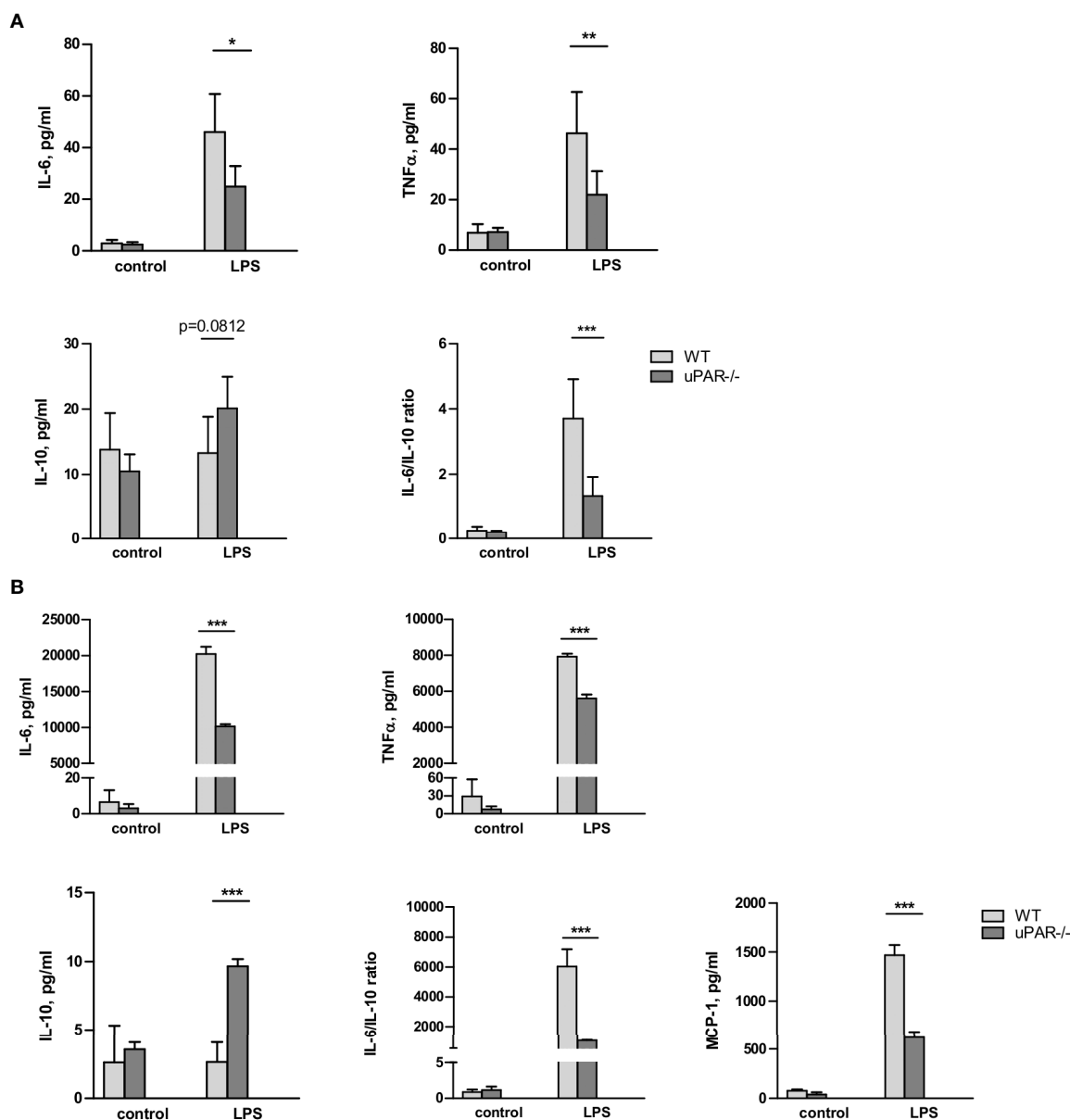
FIGURE 1 | uPAR–/– leukocytes are less responsive to LPS stimulation. **(A)** EDTA whole blood was collected from healthy WT and uPAR–/– mice (n=6 mice per group) and stimulated ex vivo with 50 ng/ml LPS for 3 h. Non-stimulated blood samples from the same animals served as controls. Cytokines response after LPS stimulation is shown. Data are presented as mean ± SD, *P < 0.05; **P < 0.01; **P < 0.001 vs. WT mice. **(B)** Peritoneal macrophages were isolated by peritoneal lavage from healthy WT and uPAR–/– mice and stimulated or not with 50 ng/ml LPS for 3 h. Cytokines response after LPS stimulation was measured in conditioned medium. Data are presented as mean ± SD from two independent experiments performed in duplicates with pooled PM isolated from n=4 mice per group, *P < 0.05; **P < 0.01; ***P < 0.001 vs. WT mice.

Together, the above data show that uPAR is involved in mediating LPS-induced effects of TLR4 in myeloid and non-myeloid cells.

uPAR Is a Part of TLR4 Interactome

Looking for possible mechanisms of uPAR interaction with TLR4 interactome, we found that addition of uPA or blocking uPA/uPAR interaction with antibody had not affected HK-2 cell response to LPS (**Supplementary Figure S2A**) suggesting that

the observed role of uPAR is independent on its plasminogen activator activity. Downregulation of uPAR expression had also minimal effect on binding of biotin-LPS by these cells as was assessed by the dot blot analysis using biotin-LPS (**Figure 5A**).

We performed duolink proximity ligation assay in HK-2 cells to assess the possibility of direct uPAR/TLR4 interaction (**Figure 5B**). The number of Duolink signal spots per cell was quantified using ImageJ Analyze particles tool. Relatively weak direct contact observed in control unstimulated cells was increased in
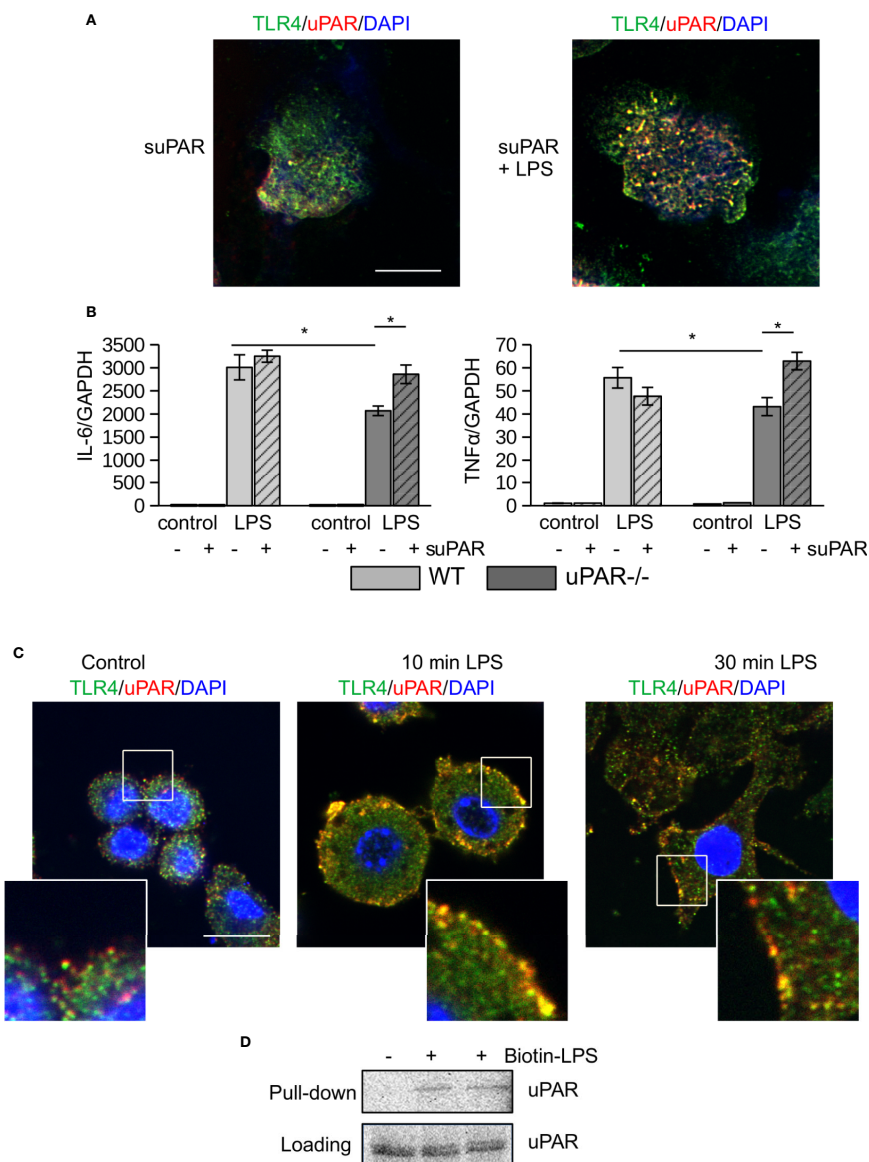
FIGURE 2 | (s)uPAR is a part of TLR4 interactome. **(A)** Primary peritoneal macrophages from uPAR−/− mice were stimulated with suPAR with or without LPS for 15 min. Then, cells were fixed and stained for TLR4 (Alexa 488, green) and uPAR (Alexa 647, red). DAPI was used as nuclear stain. Scale bar 10 µm. **(B)** Primary WT and uPAR−/− macrophages were stimulated with 50 ng/ml LPS and 1 µg/ml suPAR for 3 h. Data are presented as mean ± SD from two independent experiments performed in duplicates with pooled PM isolated from n=4 mice per group. *P < 0.05; **P < 0.01; ***P < 0.001. **(C)** Raw 264.7 cells were stimulated with 100 ng/ml LPS, fixed and stained as in A. Scale bar 12.5 µm. **(D)** Raw 264.7 cells were stimulated with 1 µg/ml biotin-LPS for 30 min, then cell lysis was performed. Protein complexes were precipitated using streptavidin magnetic beads and analyzed by western blotting using anti-murine uPAR antibody. One of 3 independent experiments with similar results is shown.

the presence of 100 ng/ml LPS (**Figure 5C**). Significantly stronger direct association detected between uPAR and CD36 in unstimulated cells was also further increased by LPS (**Figures 5B, C**). Several reports indicated that scavenger receptor CD36 can participate in LPS-induced signaling (19, 30). In our previous work we demonstrated that uPAR cooperates with TLR4 and CD36 to mediate oxLDL signaling in vascular smooth muscle

cells. To investigate whether this mechanism can function in LPS signaling, we pre-treated HK-2 cells with CD36 inhibitor SSO prior to LPS stimulation. **Figure 5D** shows that downregulation of uPAR and inhibition of CD36 decreased LPS response in HK-2 cells. However, there was no additive effect of uPARsi and CD36 inhibition suggesting that the receptors are involved in the same signaling mechanism.
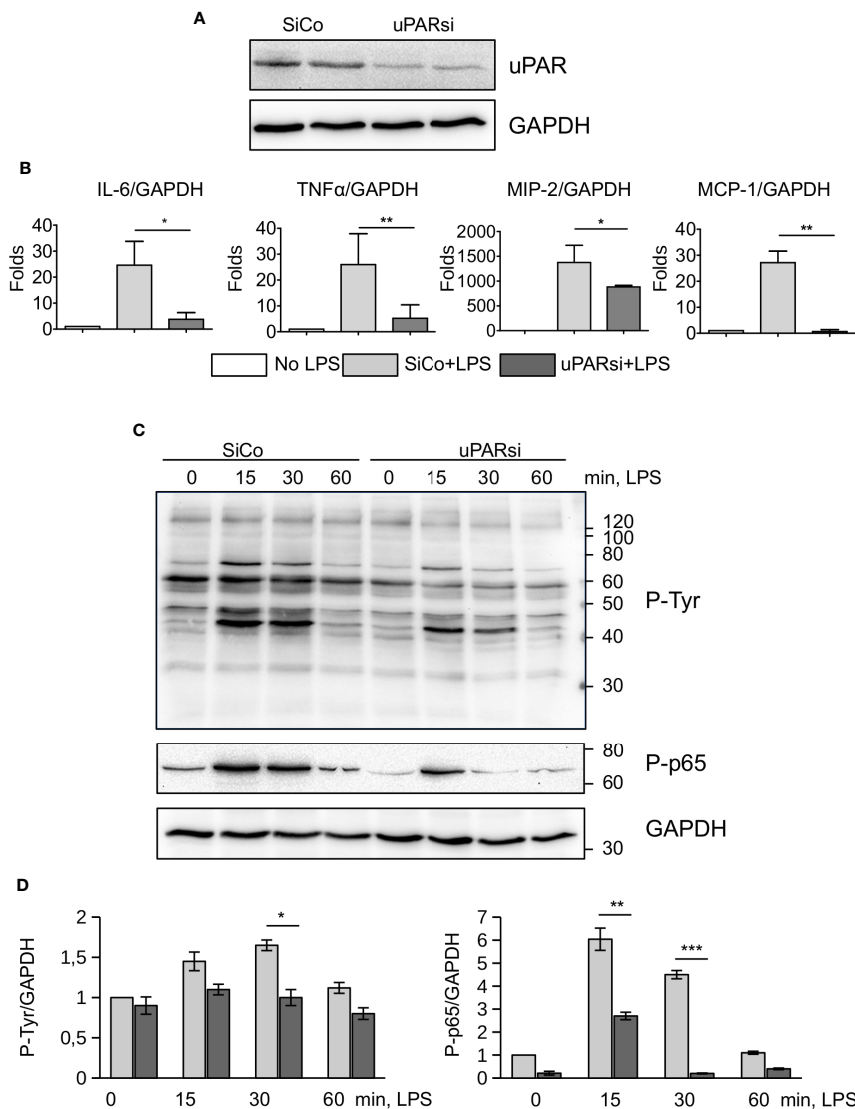
FIGURE 3 | uPAR is essential for the response of mesothelial epithelial cells to LPS. **(A)** Downregulation of uPAR expression in mouse mesothelial epithelial cells. **(B)** LPS response of SiCo and uPARsi transfected mouse mesothelial cells was assessed after stimulation with 100 ng/ml LPS for 3 h. Expression was analyzed by TaqMan RT-PCR. Data are presented as mean ± SD from three independent experiments, *P < 0.05; **P < 0.01; **P < 0.001. **(C)** LPS-induced protein tyrosine phosphorylation was assessed in SiCo and uPARsi mouse mesothelial cells by western blotting of the whole cell lysate with Ptyr antibody (upper panel) and P-p65 antibody (middle panel). GAPDH shows loading control (lower panel). **(D)** Quantification of tyrosine (left) and p65 phosphorylation (right) from three independent western blotting experiments.

Inflammatory Response of uPAR–/– Mice Is Strongly Diminished in Polymicrobial CLP Sepsis Model.

Immunohistochemical staining showed that uPAR is expressed *in vivo* in mesothelium of healthy mice whereas the expression of TLR4 was very low. After intraperitoneal (ip) injection of LPS the expression of TLR4 was strongly increased and an association between uPAR and TLR4 could be observed (**Figure 6A**) suggesting a possible involvement of uPAR into TLR4 interactome *in vivo*.

The role of uPAR in the inflammatory responses *in vivo* was further investigated in WT and uPAR–/– mice using the cecal ligation and puncture (CLP) polymicrobial sepsis model. Expression of pro-inflammatory mediators was analyzed in plasma and peritoneal lavage fluid (PL) 20 h after CLP or sham surgery. As expected, CLP-induced peritonitis was associated with a strong local and systemic up-regulation of the pro-inflammatory cytokines IL-6, MCP-1, and TNFα in WT mice. This response was strongly decreased in uPAR–/– mice by 8 and 12 folds for TNFα and MCP-1, respectively in comparison
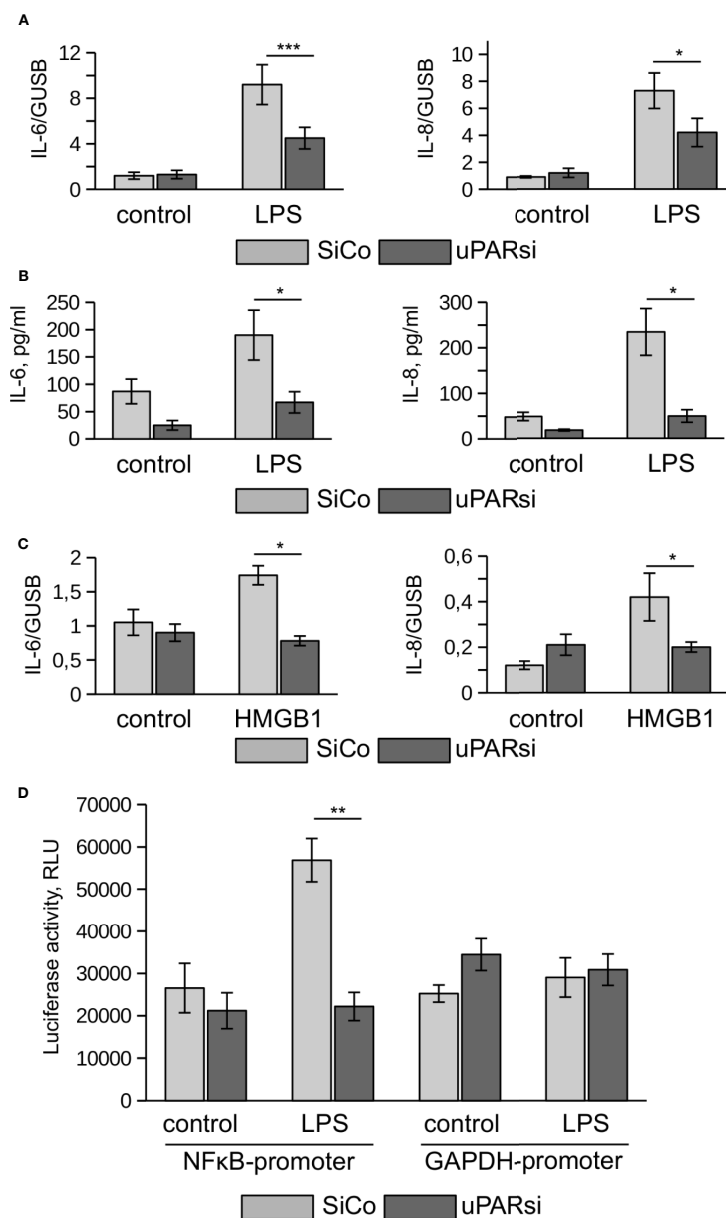
FIGURE 4 | uPAR is essential for the response of kidney proximal tubular epithelial cells to LPS. **(A, B)** LPS- induced expression of IL-6 and IL-8 by human renal proximal tubule epithelial cell (HK-2) was assessed by TaqMan RT-PCR **(A)** and ELISA **(B)**. **(C)** HMGB1-dependent IL-6 and IL-8 expression by HK-2 cells was assessed by TaqMan RT-PCR. **(D)** Human renal epithelial HK-2 cells were lentivirus-infected to express Gaussia luciferase under control of NFκB and GAPDH promoters. Enzyme activity was measured in cell conditioned media 10 h after stimulation with LPS. Data are presented as mean ± SD from three independent experiments, *P < 0.05; **P < 0.01; **P < 0.001.

to WT mice (**Figure 6B**). IL-6 expression was also low and IL-6/ IL10 ratio was also statistically significantly lower in uPAR−/− animals (**Figure 6C**). Similar decrease of expression of TNFα, MCP-1, and IL-6 was observed in peritoneal lavage fluid (PL) performed 20 h after surgery (**Figure 7A**).

To investigate whether infiltration of inflammatory cells to the peritoneum was impaired in uPAR−/− mice, we analyzed the total number of white blood cells (WBC), as well as quantified

the number of lymphocytes, monocytes, and polymorphonuclear leukocytes (PMN) in the blood and PL 20 h after surgery. The number of WBC decreased in the septic blood in both WT and uPAR−/− mice in a similar way (**Supplementary Figure 3A**). In contrast, the total inflammatory cell count in the PL fluid was increased approximately fivefold over sham controls, and this was attributable mainly to an increase in PMNs (**Figure 7B**). Similar to Renckens and colleagues (31), we have not detected
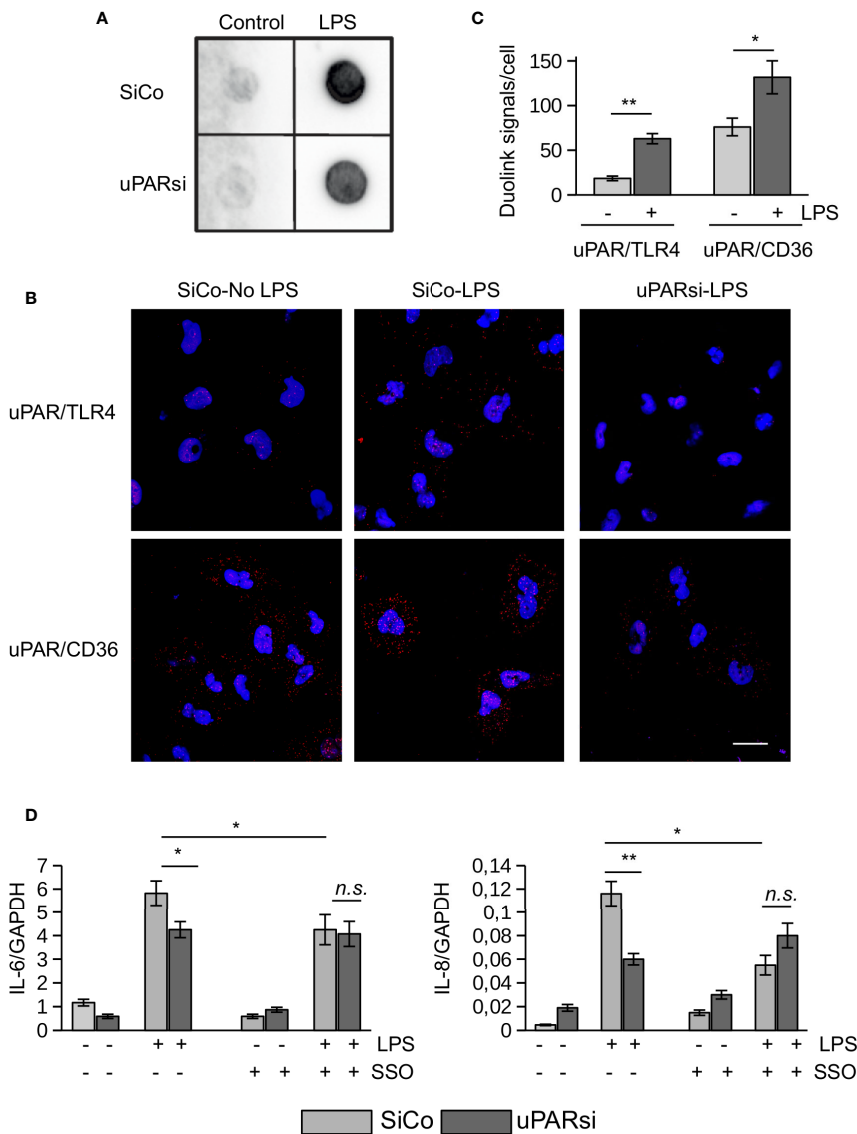
FIGURE 5 | uPAR is a part of TLR4 interactome. **(A)** Biotin-LPS binding was assessed in SiCo and uPARsi HK-2 cells as described in Methods. **(B)** Duolink proximity ligation assay to assess uPAR/TLR4 and uPAR/CD36 interaction was performed on HK-2 cells stimulated with 100 ng/ml LPS for 15 min as described in Methods. **(C)** Duolink images were quantified using Particles analysis tool of ImageJ. **(D)** HK-2 cells were stimulated with 100 ng/ml LPS for 3 h after cell pre-treatment with 10 µM of CD36 inhibitor SSO. Expression of IL-6 and IL-8 was assessed by TaqMan RT-PCR. Data are presented as mean ± SD from three independent experiments, *P < 0.05; **P < 0.01; **P < 0.001; n.s. not significant.

significant deviation in the number of infiltrating inflammatory cells in the peritoneum of uPAR−/− mice in comparison to WT 20 h after CLP surgery (**Figure 7B**).

Further, we analyzed bacterial load in PL of WT and uPAR−/− mice 20 h after CLP surgery. Our data showed that though lower number of bacteria was found in PL of uPAR−/− animals, these differences has not reached statistical significance in comparison with WT mice (**Figure 7C**). Further, we analyzed capacity of uPAR−/− peritoneal macrophages to phagocytose FITC-labeled *E. coli* (**Figure 7D**). Phagocytic capacity of both, untreated uPAR−/−

macrophages and cells treated with PL was lower than in WT macrophages.

Confirming diminished development of inflammatory response, kidney function was significantly improved in uPAR−/− mice. Thus, blood level of creatinine was strongly increased in septic WT mice but remained at the normal level in uPAR−/− mice (**Figure 8A**). The level of blood urea nitrogen (BUN) was also significantly diminished in septic uPAR−/− mice compared to WT animals. Liver dysfunction was assessed on the basis of enzymatic activities of circulating liver enzymes glutamate
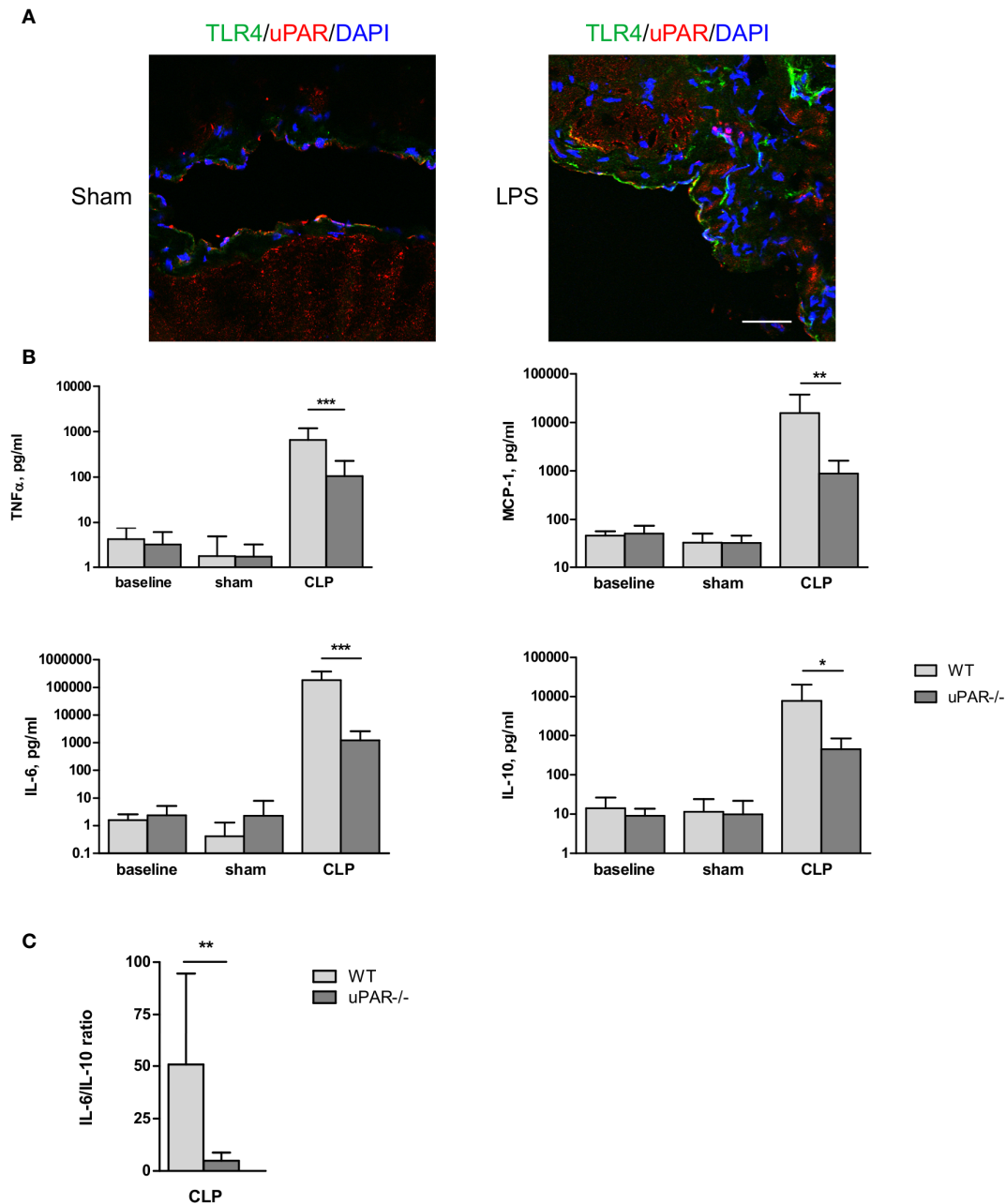
FIGURE 6 | Effect of uPAR deficiency on systemic inflammatory response in polymicrobial sepsis model. **(A)** Peritoneum of sham and LPS-injected WT mice was fixed and stained for uPAR (red) and TLR4 (green). DAPI used as nuclear stain. Scale bar 100 μm. **(B)** High-grad sepsis was induced in WT and uPAR−/− mice by CLP surgery with ligation of 75% of the cecum length (n=10 mice per group). Sham operated mice served as controls (n=6 mice per group). Blood sample were obtained at 20 h after surgery and inflammatory response was evaluated by cytokine measurements in plasma. **(C)** IL-6/IL-10 ratio in plasma of WT and uPAR−/− septic mice. Data in are presented as mean ± SD, *P < 0.05; **P < 0.01; **P < 0.001 vs. WT mice.

oxaloacetate transaminase/aspartate glutaminase (GOT/AST) and glutamate pyruvate transaminase/alanine aminotransferase (GPT/ALT) (32). Both, GOT and GPT levels were also lower in uPAR−/− septic mice in comparison to WT animals (**Figure 8B**). Plasma level of lactate dehydrogenase (LDH) reflecting the degree of overall tissue damage was also strongly decreased in uPAR−/− mice (**Figure 8C**). Basal levels of creatinine, BUN, GOT/AST

and GPT/ALT as well as LDH were similar between WT and uPAR−/− mice (baseline in **Figures 8A–C**). In agreement with decreased inflammatory response and improved organ function, uPAR−/− mice demonstrated much better survival in CLP model than WT animals (**Figure 8D**). All sham-operated mice (n=6 per group) survived for the period of observation (data not shown).
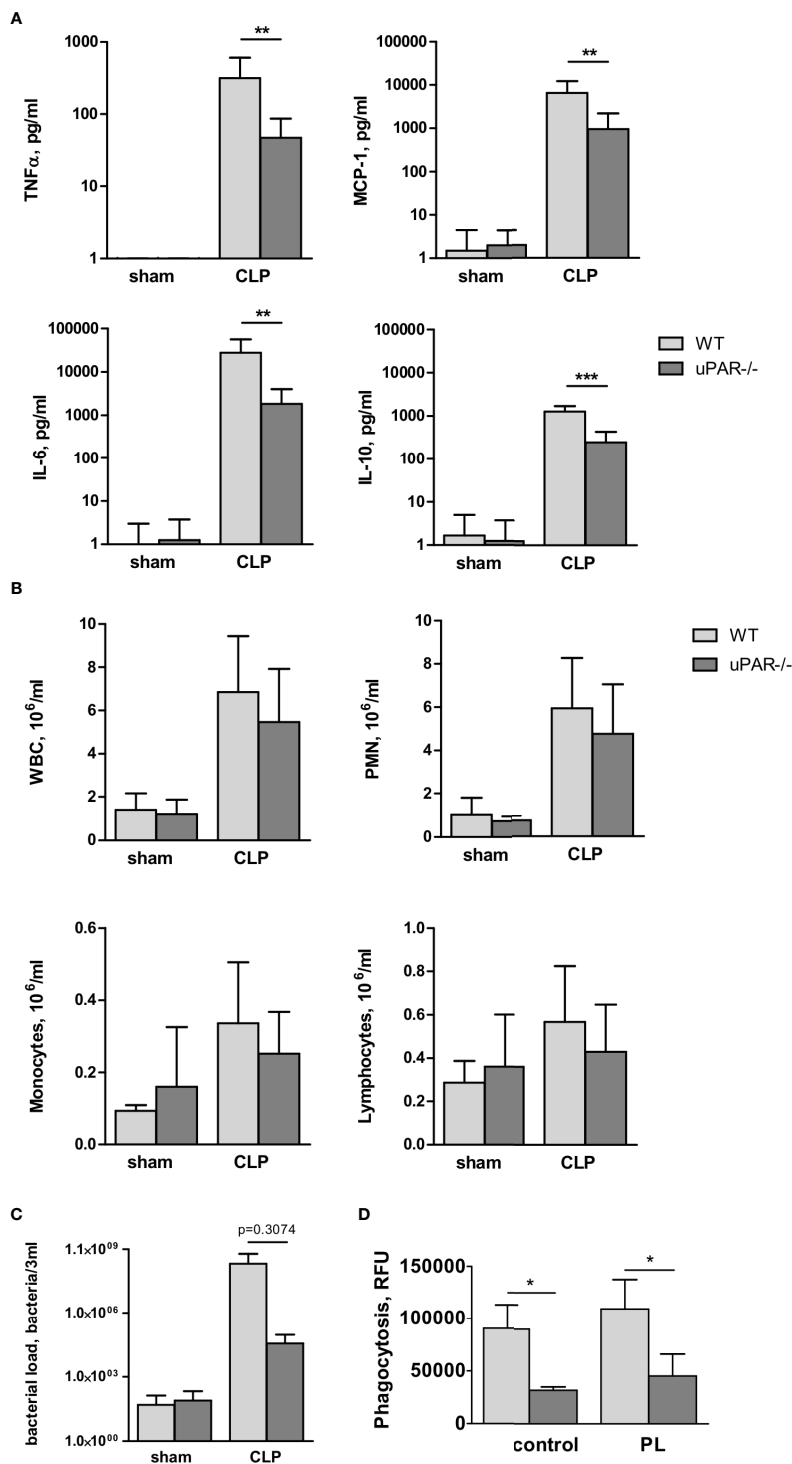
FIGURE 7 | Effect of uPAR deficiency on local inflammatory response in polymicrobial sepsis model. High-grad sepsis was induced in WT and uPAR–/– mice as described above (n=10 mice per group). Sham operated mice served as controls (n=6 mice per group). Peritoneal lavage was performed at 20 h after surgery and inflammatory response was evaluated by cytokine measurement and inflammatory cell population analysis. **(A)** CLP-induced cytokine release in PL. **(B)** White blood cell (WBC) counts and differential cell counts from PL samples at 20 h after CLP or sham operation (n=6 to 10 mice per group).. *P < 0.05; **P < 0.01; **P < 0.001. PMN, polymorphonuclear neutrophils. **(C)** Bacterial load in PL of WT and uPAR–/– mice was assessed by plating serial dilutions of PL fluid on Columbia blood-agar base plates. **(D)** Phagocytic capacity of WT and uPAR–/– naïve peritoneal macrophages and cells treated overnight with PL obtained from CLP-WT mice was assessed using FITC-labelled *E. Coli.* Data in are presented as mean ± SD, *P < 0.05; **P < 0.01; **P < 0.001 vs. WT mice.
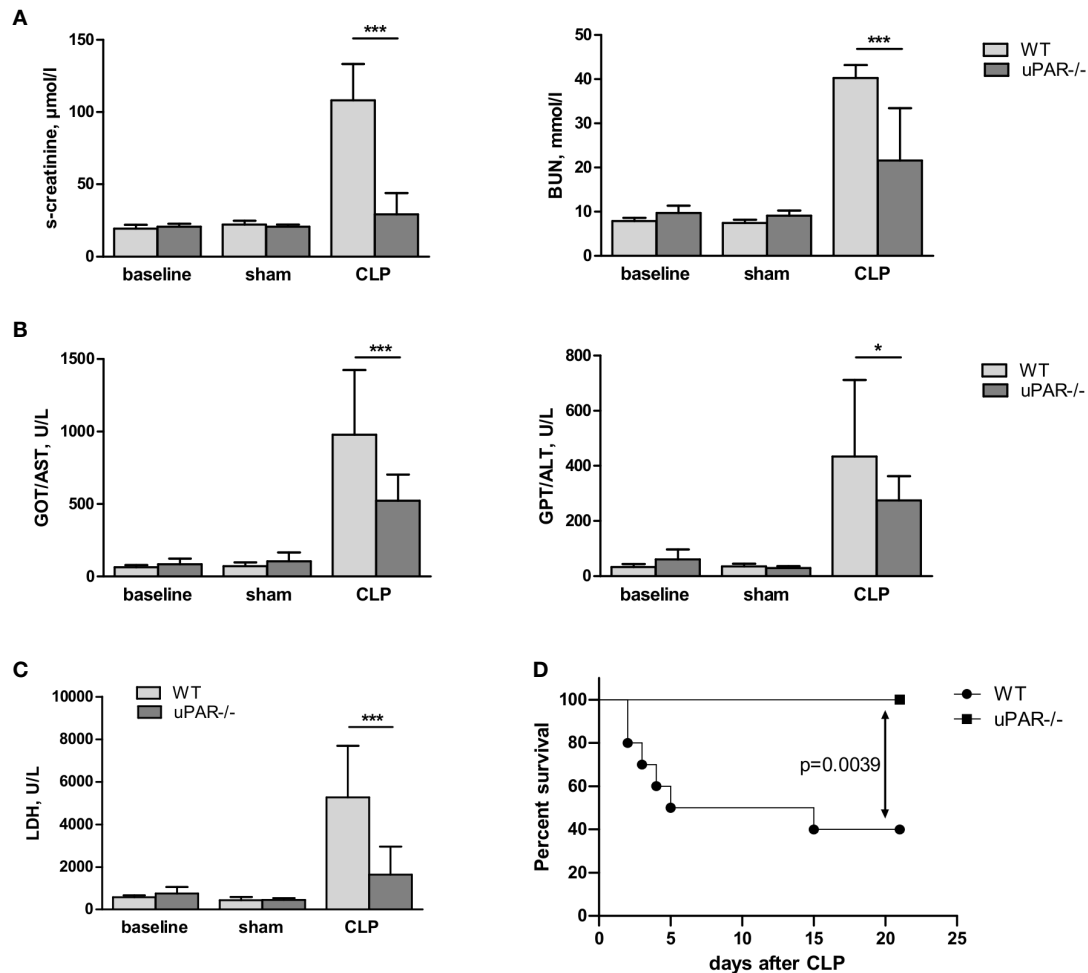
FIGURE 8 | Effect of uPAR deficiency on multiorgan failure and survival in polymicrobial sepsis model. High-grad sepsis was induced in WT and uPAR−/− mice by CLP surgery as described in above (n= 10 mice per group). Sham operated mice served as controls (n=6 mice per group). **(A)** Kidney function was estimated by the measurements of serum creatinine and blood urea nitrogen (BUN) levels at 20 h after CLP or sham surgery. **(B)** Liver function was estimated by the measurements of AST and ALT levels. **(C)** Serum lactate dehydrogenase (LDH) levels were determined 20 h after sham or CLP surgery. Data are presented as mean ± SD, *P < 0.05; **P < 0.01; **P < 0.001 vs. WT mice. **(D)** Mid-grade sepsis was induced in WT and uPAR−/− mice by CLP surgery with ligation of 50% of the cecum length (n= 10 mice per group). Survival was monitored daily for 21 days, Kaplan-Mayer curves were generated and Gehan-Breslow-Wilcoxon test was performed for statistical analysis.

DISCUSSION

In this study we demonstrated that uPAR promotes TLR4-mediated response to LPS in myeloid and non-myeloid cells. Using different approaches, we showed that GPI-uPAR and suPAR can integrate into TLR4 interactome and promote cell signaling leading to the secretion of cytokines and chemokines.

The role of uPAR in immunity is multifaceted and mechanisms are not completely understood. Well-documented is the involvement of uPAR in the migration of inflammatory cells. Migration of granulocytes to the lungs upon pneumococcal pneumonia was impaired in uPAR−/− mice (10). This was accompanied by increased bacterial load and higher mortality. Similar impairment of neutrophil migration to the lung was also reported upon *Pseudomonas aeruginosa* infection (11). This was

also accompanied by diminished bacterial clearance. Another study showed that during borellia burgdorferi skin infection, the number of spirochetes was increased in uPAR−/− mice (33). However, in that case infiltration of macrophages was higher in uPAR−/− mice and the effect was attributed to the impaired phagocytosis of bacteria. The mechanisms of uPAR involvement may include regulation of proteolysis on the leading edge of migrating cell (34) chemotaxis and activation of immune cells (35), due to uPAR interactions with cell surface partners, as integrins and the chemotaxis fMLF-receptors (36). In addition, uPAR occupation by inactive uPA or its amino terminal fragment may regulate several activities, including cell adhesion and migration (1).

Non-proteolytic effects of uPAR on innate immunity were investigated by Liu et al (13). during *in vitro* stimulation of uPAR−/− granulocytes with TLR2 and TLR4 ligands. They

showed that uPAR is essential for cell response to TLR2 ligand. The mRNA expression was not decreased, however, release of IL-6 and TNFα was diminished in uPAR−/− cells. The authors also stimulated uPAR−/− granulocytes with TLR4 ligand LPS and observed no changes in mRNA expression of IL-6 and TNFα after 24 h of stimulation. On the contrary, in our experiments we demonstrated diminished mRNA expression of LPS-induced inflammatory mediators in different cell types after downregulation of uPAR. The discrepancy with the data by Liu et al. can be explained by different stimulation conditions. In our experiments stimulation with LPS for 3 h was found optimal to assess changes of mRNA expression. Changes of protein expression were pronounced 24 h after treatment, whereas the changes of RNA expression were no longer visible at that time point. Similar to Liu and colleagues, in our experiments TLR1 and TLR1/2 ligands PAM3CSK4 and lipoteichoic acid (LTA) also induced less inflammatory response in uPARsi cells (data not shown).

Our data showed that uPAR interferes with signaling of TLR4 to different PAMP and DAMP molecules. We also found uPAR to be a part of TLR4 interactome. Interestingly, suPAR also interacted with TLR4 and promoted LPS signaling in uPAR−/− cells. These data suggest that regulation of LPS response of TLR4 by (s)uPAR depends on the availability of membrane-bound and soluble uPAR. LPS signaling of TLR4 is very complex. In addition to CD14 and MD2 co-receptors, recent data demonstrated that TLR4 can recruit further membrane receptors such as TLR2, CD36, integrin CD11b, heat shock proteins and others (37). Looking for possible mechanisms of uPAR effects, we showed that these effects were not dependent on uPA/uPAR interaction. Rather, TLR4 or uPAR interaction with common co-receptors was affected. Recent report showed that LPS-dependent signaling and expression of inflammatory mediators was decreased after silencing CD36 in epithelial cells (30). Accordingly, we showed that inhibition of CD36 decreases LPS response in SiCo but not in uPARsi HK-2 cells, suggesting that uPAR and CD36 are involved in the same molecular mechanism. So, it is possible that uPAR mediates LPS-dependent TLR4/CD36 cross-talk in a similar fashion as we have previously demonstrated for oxLDL signaling (18). This hypothesis is strengthened by our observation that expression of uPAR did not promote LPS response in HEK-BlueTLR4 reporter cell line (Invivogen) – HEK 293 cells that stably express TLR4, CD14, and MD-2. It is recognized that transcriptome of HEK 293 is specific and the cells do not express a variety of scavenger receptors and PRRs. This data suggest that fine mechanisms of (s)uPAR interference is probably cell type dependent, depend on the ligand nature, and can be fine-tuned by the availability of various co-receptors, and further factors.

In vivo in CLP mouse polymicrobial sepsis model we found that uPAR−/− mice demonstrate much better survival in comparison to WT animals. The levels of TNFα, MCP-1, and IL-6 in PL fluid and in blood plasma of uPAR−/− mice were significantly lower. Interestingly, recruitment of innate immunity cells to the peritoneum was similar between uPAR−/− and WT mice 20 h after surgery. This data is in agreement with the report by Renckens et al. (31), who showed that LPS-dependent migration after ip LPS injection was impaired in uPAR−/− mice, whereas the effects were compensated upon sepsis induction by the injection of living *E. coli*. Similar to Hovius et al. (33) we found that capacity of uPAR−/− macrophages to phagocytose bacteria was decreased. The number of bacteria in PL of uPAR−/− mice assessed 20 h after CLP surgery was lower than in WT animals, though these differences were not statistically significant. This trend can be explained by faster protective fibrotic response in uPAR−/− mice (38) or different composition of gut microbiome in WT and uPAR−/− mice (39, 40). This issue requires further investigation to enable therapeutic targeting of uPAR-dependent methanisms in sepsis,

Importantly, we also found that plasma content of LDH indicating overall tissue damage in sepsis was strongly decreased in uPAR−/− mice. Kidney and liver function were also improved as was assessed by the plasma content of creatinine, BUN, AST, and ALT. It should be kept in mind that CLP is a very severe sepsis model where inflammation is induced by combination of gram-positive and gram-negative bacteria that can be recognized by many pattern recognition receptors. An important role of TLR4 in this process was confirmed by the observation of Chen et al. who showed that TLR4−/− mice demonstrated improved survival and decreased level of cytokines after CLP (41). Knockdown of CD14 that functions not only with TLR4 but also with other TLRs had even stronger protective effect in mouse CLP model (42). Our data show that uPAR that can interfere with PRRs signaling and thus promote immune response. This mechanism represents a potentially important target in sepsis therapy. Further research is needed to identify uPAR interaction partner-PRR and develop a strategy to target this interaction.

DATA AVAILABILITY STATEMENT

The raw data supporting the conclusions of this article will be made available by the authors, without undue reservation.

ETHICS STATEMENT

The animal study was reviewed and approved by Lower Saxony Office for Consumer Protection and Food Safety; P.O. Box 3949, 26029 Oldenburg, Germany.

AUTHOR CONTRIBUTIONS

Study design: YK, AG, PR, ID, HH, NS. Experimental work: YK, ST, AG, NS, SR. Manuscript preparation: all authors. All authors contributed to the article and approved the submitted version.

SUPPLEMENTARY MATERIAL

The Supplementary Material for this article can be found online at: https://www.frontiersin.org/articles/10.3389/fimmu.2020.573550/full#supplementary-material

REFERENCES

1. Smith HW, Marshall CJ. Regulation of cell signalling by uPAR. *Nat Rev Mol Cell Biol* (2010) 11:23–36. doi: 10.1038/nrm2821
2. Mahmood N, Mihalcioiu C, Rabbani SA. Multifaceted Role of the Urokinase-Type Plasminogen Activator (uPA) and Its Receptor (uPAR): Diagnostic, Prognostic, and Therapeutic Applications. *Front Oncol* (2018) 8:24. doi: 10.3389/fonc.2018.00024
3. Montuori N, Pesapane A, Rossi FW, Giudice V, De Paulis A, Selleri C, et al. Urokinase type plasminogen activator receptor (uPAR) as a new therapeutic target in cancer. *Transl Med @ UniSa* (2016) 15:15–21.
4. Narayanaswamy PB, Baral TK, Haller H, Dumler I, Acharya K, Kiyan Y. Transcriptomic pathway analysis of urokinase receptor silenced breast cancer cells: A microarray study. *Oncotarget* (2017) 8:101572–90. doi: 10.18632/oncotarget.21351
5. Dergilev KV, Stepanova VV, Beloglazova IB, Tsokolayev ZI, Parfenova EV. Multifaced Roles of the Urokinase System in the Regulation of Stem Cell Niches. *Acta Naturae* (2018) 10:19–32. doi: 10.32607/20758251-2018-10-4-19-32
6. Motta C, Lupo G, Rusciano D, Olivieri M, Lista L, De Rosa M, et al. Molecular Mechanisms Mediating Antiangiogenic Action of the Urokinase Receptor-Derived Peptide UPARANT in Human Retinal Endothelial Cells. *Invest Ophthalmol Vis Sci* (2016) 57:5723–35. doi: 10.1167/iovs.16-19909
7. Long D, Yang J, Wu X, Gui Y, Yu L. Urokinase-type plasminogen activator protects human umbilical vein endothelial cells from apoptosis in sepsis. *Int J Clin Exp Pathol* (2019) 12:77–86.
8. Shushakova N, Eden G, Dangers M, Menne J, Gueler F, Luft FC, et al. The urokinase/urokinase receptor system mediates the IgG immune complex-induced inflammation in lung. *J Immunol* (2005) 175:4060–8. doi: 10.4049/jimmunol.175.6.4060
9. Gueler F, Rong S, Mengel M, Park JK, Kiyan J, Kirsch T, et al. Renal urokinase-type plasminogen activator (uPA) receptor but not uPA deficiency strongly attenuates ischemia reperfusion injury and acute kidney allograft rejection. *J Immunol* (2008) 181:1179–89. doi: 10.4049/jimmunol.181.2.1179
10. Rijneveld AW, Levi M, Florquin S, Speelman P, Carmeliet P, van Der Poll T. Urokinase receptor is necessary for adequate host defense against pneumococcal pneumonia. *J Immunol* (2002) 168:3507–11. doi: 10.4049/jimmunol.168.7.3507
11. Gyetko MR, Sud S, Kendall T, Fuller JA, Newstead MW, Standiford TJ. Urokinase receptor-deficient mice have impaired neutrophil recruitment in response to pulmonary Pseudomonas aeruginosa infection. *J Immunol* (2000) 165:1513–9. doi: 10.4049/jimmunol.165.3.1513
12. Kang SS, Sim JR, Yun CH, Han SH. Lipoteichoic acids as a major virulence factor causing inflammatory responses via Toll-like receptor 2. *Arch Pharm Res* (2016) 39:1519–29. doi: 10.1007/s12272-016-0804-y
13. Liu G, Yang Y, Yang S, Banerjee S, De Freitas A, Friggeri A, et al. The receptor for urokinase regulates TLR2 mediated inflammatory responses in neutrophils. *PloS One* (2011) 6:e25843. doi: 10.1371/journal.pone.0025843
14. Singer M, Deutschman CS, Seymour CW, Shankar-Hari M, Annane D, Bauer M, et al. The Third International Consensus Definitions for Sepsis and Septic Shock (Sepsis-3). *JAMA* (2016) 315:801–10. doi: 10.1001/jama.2016.0287
15. Rello J, Valenzuela-Sanchez F, Ruiz-Rodriguez M, Moyano S. Sepsis: A Review of Advances in Management. *Adv Ther* (2017) 34:2393–411. doi: 10.1007/s12325-017-0622-8
16. Chen D, Wu X, Yang J, Yu L. Serum plasminogen activator urokinase receptor predicts elevated risk of acute respiratory distress syndrome in patients with sepsis and is positively associated with disease severity, inflammation and mortality. *Exp Ther Med* (2019) 18:2984–92. doi: 10.3892/etm.2019.7931
17. Zhao JJ, Lou XL, Chen HW, Zhu FT, Hou YQ. Diagnostic value of decoy receptor 3 combined with procalcitonin and soluble urokinase-type plasminogen activator receptor for sepsis. *Cell Mol Biol Lett* (2018) 23:22. doi: 10.1186/s11658-018-0087-z
18. Kiyan Y, Tkachuk S, Hilfiker-Kleiner D, Haller H, Fuhrman B, Dumler I. OxLDL induces inflammatory responses in vascular smooth muscle cells via urokinase receptor association with CD36 and TLR4. *J Mol Cell Cardiol* (2014) 66:72–82. doi: 10.1016/j.yjmcc.2013.11.005
19. Biedroń R, Peruń A, Józefowski S. CD36 Differently Regulates Macrophage Responses to Smooth and Rough Lipopolysaccharide. *PloS One* (2016) 2016) 11:e0153558. doi: 10.1371/journal.pone.0153558
20. Means TK, Golenbock DT, Fenton MJ. The biology of Toll-like receptors. *Cytokine Growth Factor Rev* (2000) 11:219–32. doi: 10.1016/s1359-6101(00)00006-x
21. Wang L, Balzer MS, Rong S, Menne J, Vietinghoff S, Dong L, et al. Protein kinase C alpha inhibition prevents peritoneal damage in a mouse model of chronic peritoneal exposure to high-glucose dialysate. *Kidney Int* (2016) 89:1253–67. doi: 10.1016/j.kint.2016.01.025
22. Balzer MS, Helmke A, Ackermann M, Casper J, Dong L, Hiss M, et al. Protein kinase C beta deficiency increases glucose-mediated peritoneal damage via M1 macrophage polarization and up-regulation of mesothelial protein kinase C alpha. *Nephrol Dial Transplant* (2019) 34:947–60. doi: 10.1093/ndt/gfy282
23. Kümpers P, Gueler F, David S, Van Slyke P, Dumont DJ, Park JK, et al. The synthetic Tie2 agonist peptide vasculotide protects against vascular leakage and reduces mortality in murine abdominal sepsis. *Crit Care* (2011) 15:R261. doi: 10.1186/cc10523
24. Rittirsch D, Huber-Lang MS, Flierl MA, Ward PA. Immunodesign of experimental sepsis by cecal ligation and puncture. *Nat Protoc* (2009) 2009) 4:31–6. doi: 10.1038/nprot.2008.214
25. Segre E, Fullerton JN. Stimulated Whole Blood Cytokine Release as a Biomarker of Immunosuppression in the Critically Ill: The Need for a Standardized Methodology. *Shock* (2016) 45:490–4. doi: 10.1097/SHK.0000000000000557
26. Yoshimura T, Galligan C, Takahashi M, Chen K, Liu M, Tessarollo L, et al. Non-Myeloid Cells are Major Contributors to Innate Immune Responses via Production of Monocyte Chemoattractant Protein-1/CCL2. *Front Immunol* (2014) 4:482. doi: 10.3389/fimmu.2013.00482
27. Kato S, Yuzawa Y, Tsuboi N, Maruyama S, Morita Y, Matsuguchi T, et al. Endotoxin-induced chemokine expression in murine peritoneal mesothelial cells: the role of toll-like receptor 4. *J Am Soc Nephrol* (2004) 15:1289–99.
28. Ragnarsdottir B, Lutay N, Gronberg-Hernandez J, Koves B, Svanborg C. Genetics of innate immunity and UTI susceptibility. *Nat Rev Urol* (2011) 8:449–68. doi: 10.1038/nrurol.2011.100
29. Zheng S, Pan Y, Wang C, Liu Y, Shi M, Ding G. HMGB1 Turns Renal Tubular Epithelial Cells into Inflammatory Promoters by Interacting with TLR4 During Sepsis. *J Interferon Cytokine Res* (2016) 36:9–19. doi: 10.1089/jir.2015.0067
30. Cao D, Luo J, Chen D, Xu H, Shi H, Jing X, et al. CD36 regulates lipopolysaccharide-induced signaling pathways and mediates the internalization of Escherichia coli in cooperation with TLR4 in goat mammary gland epithelial cells. *Sci Rep* (2016) 6:23132. doi: 10.1038/srep23132

31. Renckens R, Roelofs JJTH, Florquin S, van der Poll T. Urokinase-type plasminogen activator receptor plays a role in neutrophil migration during lipopolysaccharide-induced peritoneal inflammation but not during Escherichia coli-induced peritonitis. *J Infect Dis* (2006) 193:522–30. doi: 10.1086/499601

32. Huang LJ, Dong HP, Chuang IC, Liu MS, Yang RC. Attenuation of mitochondrial unfolded protein response is associated with hepatic dysfunction in septic rats. *Shock* (2012) 38:642–8. doi: 10.1097/SHK.0b013e3182734ff9

33. Hovius JWR, Bijlsma MF, van der Windt GJW, Wiersinga WJ, Boukens BJD, Coumou J, et al. The urokinase receptor (uPAR) facilitates clearance of Borrelia burgdorferi. *PloS Pathog* (2009) 5:e1000447. doi: 10.1371/journal.ppat.1000447

34. Fleetwood AJ, Achuthan A, Schultz H, Nansen A, Almholt K, Usher P, et al. Urokinase plasminogen activator is a central regulator of macrophage three-dimensional invasion, matrix degradation, and adhesion. *J Immunol* (2014) 192:3540–7. doi: 10.4049/jimmunol.1302864

35. Del Rosso M, Margheri F, Serrati S, Chilla A, Laurenzana A, Fibbi G. The urokinase receptor system, a key regulator at the intersection between inflammation, immunity, and coagulation. *Curr Pharm Des* (2011) 17:1924–43. doi: 10.2174/138161211796718189

36. Gorrasi A, Li Santi A, Amodio G, Alfano D, Remondelli P, Montuori N, et al. The urokinase receptor takes control of cell migration by recruiting integrins and FPR1 on the cell surface. *PloS One* (2014) 9:e86352. doi: 10.1371/journal.pone.0086352

37. Plociennikowska A, Hromada-Judycka A, Borzecka K, Kwiatkowska K. Co-operation of TLR4 and raft proteins in LPS-induced pro-inflammatory signaling. *Cell Mol Life Sci* (2015) 72:557–81. doi: 10.1007/s00018-014-1762-5

38. Kanno Y, Kaneiwa A, Minamida M, Kanno M, Tomogane K, Takeuchi K, et al. The absence of uPAR is associated with the progression of dermal fibrosis. *J Invest Dermatol* (2008) 128:2792–7. doi: 10.1038/jid.2008.157

39. Alegre ML. Mouse microbiomes: overlooked culprits of experimental variability. *Genome Biol* (2019) 20:108. doi: 10.1186/s13059-019-1723-2

40. Korach-Rechtman H, Freilich S, Gerassy-Vainberg S, Buhnik-Rosenblau K, Danin-Poleg Y, Bar H, et al. Murine Genetic Background Has a Stronger Impact on the Composition of the Gut Microbiota than Maternal Inoculation or Exposure to Unlike Exogenous Microbiota. *Appl Environ Microbiol* (2019) 85:e00826–19. doi: 10.1128/AEM.00826-19

41. Chen X, Wang T, Song L, Liu X. Activation of multiple Toll-like receptors serves different roles in sepsis-induced acute lung injury. *Exp Ther Med* (2019) 18:443–50. doi: 10.3892/etm.2019.7599

42. Chen Z, Ding X, Jin S, Pitt B, Zhang L, Billiar T, et al. WISP1-alphavbeta3 integrin signaling positively regulates TLR-triggered inflammation response in sepsis induced lung injury. *Sci Rep* (2016) 6:28841. doi: 10.1038/srep28841

43. Kiyan Y, Tkachuk S, Gorrasi A, Ragno P, Dumler I, Haller H, et al. Urokinase receptor associates with TLR4 interactome to promote LPS response. *BioRxiv* (2020). doi: 10.1101/2020.06.10.143826. 2020.06.10.143826.